Search for supersymmetry using boosted Higgs bosons and missing transverse momentum in proton-proton collisions at 13 TeV

by

Frank Jensen

M.S., University of Colorado Boulder, 2014

B.A., University of California Berkeley, 2008

A thesis submitted to the

Faculty of the Graduate School of the

University of Colorado in partial fulfillment

of the requirements for the degree of

Doctor of Philosophy

Department of Physics

2018

This thesis entitled:
Search for supersymmetry using boosted Higgs bosons and missing transverse momentum in proton-proton collisions at 13 TeV
written by Frank Jensen
has been approved for the Department of Physics

Professor Kevin Stenson

Professor William Ford

Professor Jamie Nagle

Date

The final copy of this thesis has been examined by the signatories, and we find that both the content and the form meet acceptable presentation standards of scholarly work in the above mentioned discipline.

Jensen, Frank (Ph.D.,experiment high-energy physics)

Search for supersymmetry using boosted Higgs bosons and missing transverse momentum in proton-proton collisions at 13 TeV

Thesis directed by Professor Kevin Stenson

A search for physics beyond the standard model in events with one or more high-momentum Higgs bosons, H, decaying to pairs of b quarks in association with missing transverse momentum is presented. The data, corresponding to an integrated luminosity of $35.9\,\mathrm{fb}^{-1}$, were collected with the CMS detector at the LHC in proton-proton collisions at the center-of-mass energy $\sqrt{s} = 13\,\mathrm{TeV}$. The analysis utilizes a new b quark tagging technique based on jet substructure to identify jets from $\mathrm{H} \to b\bar{b}$. Events are categorized by the multiplicity of H-tagged jets, jet mass, and the missing transverse momentum. No significant deviation from standard model expectations is observed. In the context of supersymmetry (SUSY), limits on the cross sections of pair-produced gluinos are set, assuming that gluinos decay to quark pairs, H (or Z), and the lightest SUSY particle, LSP, through an intermediate next-to-lightest SUSY particle, NLSP. With large mass splitting between the NLSP and LSP, and 100% NLSP branching fraction to H, the lower limit on the gluino mass is found to be 2010 GeV.

Dedications & Acknowledgements

The section with the dedications and acknowledgements.

Contents

Tables

Figures

Chapter 1

Introduction

A description of the Standard Model is presented in Chapter **??**. A description of the CMS detector is presented in Chapter **??**. The physics analysis which serves as the foundation of the thesis work is presented in Chapter **??**. Work done since the conclusion of the analysis on the commissioning of the $b\bar{b}$-tagging in data produced in 2017 is described in **??**.

Chapter 2

The Standard Model of Particle Physics

A section describing the Standard Model of particle physics.

Chapter 3

The CMS Detector

The detector is cylindrically symmetric, with a modular design consisting of different subsystems each specialized for detection or identification of specific particles. Many of the Standard Model particles are unstable. In fact only about 8 particles are directly detected in our experiment, the rest of those being reconstructed via their decay into these more stable elements. Of all the Standard Model particles,

Figure **??** is a depiction of the CMS detector. Figure **??** is a schematic view of the CMS detector and the particles it interacts with.

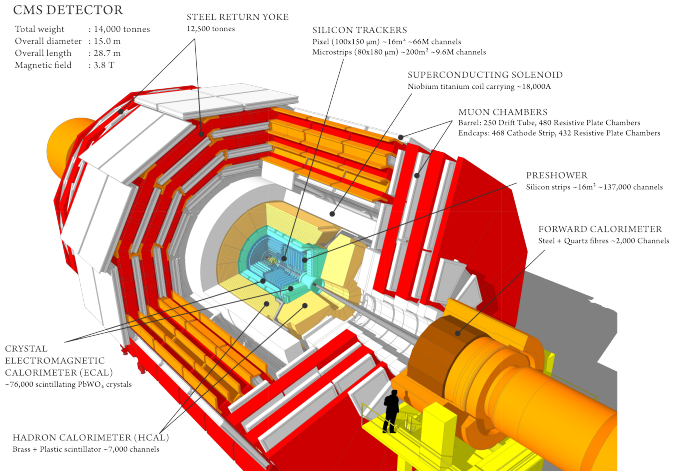

Figure 3.1: A depiction of the CMS detector.

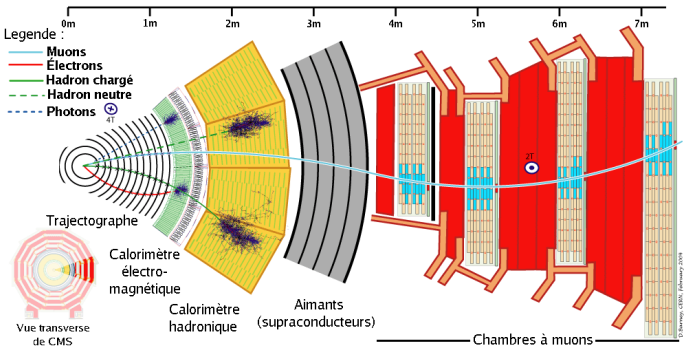

Figure 3.2: A schematic view of the CMS detector and the particles it interacts with.

3.1 Silicon Tracker

At the center of the detector lies the silicon tracker which is responsible for momentum reconstruction of charged particles and reconstruction of the primary vertices created from a proton-proton interaction. The tracker is composed of a number of concentric cylindrical layers each instrumented with silicon sensors. As a charged particle traverses an individual sensor a small amount of ionization energy is deposited in that element. A bias voltage is applied across the sensor to direct the charge to either end of the sensor. Bonded to the sensors are front-end electronics responsible for the amplification and shaping of the resultant signal. Neighboring elements are clustered together creating what is known as a "hit". These hits are then used to reconstruct the particle's trajectory through the tracker. To make a measurement of the momentum and charge of the particle, the tracker is immersed in a 3.8 T magnetic field which bends the trajectory of the particle.

The tracker is further divided into an inner and outer parts which make use of slightly different technologies. The inner part of the tracker is known as the pixel detector and consists of 4 layers which the sensitive elements are silicon pixels of size 100x150 μm. This fine granularity of

Chapter 4

Analysis

4.1 Introduction

As the search for Supersymmetry continues to come up empty handed, the masses of potentially new particles are pushed to larger and larger scales. One consequence is that the Standard Model particles radiated in their decay should have correspondingly larger and larger momentum. As the momentum of a particle becomes larger the decay products tend to be emitted at smaller angles, eventually reaching the point where we could reconstruct all the decay objects within a single "fat jet" reconstructed using the "anti-kt" algorithm with a cone size parameter 0.8 [**?**]. We present an analysis searching for hints of new physics beyond the Standard Model in events with one or two Higgs bosons and a large imbalance in the transverse momentum resulting from supersymmetric particles escaping detection. We require the Higgs boson to decay to b-quarks, exploiting the large (57%) branching fraction to b-quarks. The branching fraction of Z bosons to b-quarks is substantially smaller at 15%. This analysis is documented in [**?**] and built heavily on previously published work [**?**] [**?**]. To further suppress misidentification of these jets, we further require the invariant mass of the jet to be consistent with the Higgs boson, to improve mass reconstruction, the soft and wide angle radiation is first removed from the jet before the mass calculation. A process known as pruning [**?**].

4.2 Event & Object Selection

Although our analysis is sensitive to any process which can produce boosted Higgs or Z bosons, we have adopted a couple of benchmark models, seen in Figure **??**, to give motivation to the region of phase space we work in. In this scenario, the proton-proton interaction produces a pair of gluinos ($\tilde{g}$) which decay to a neutralino (χ_2^0) by the emission of Standard Model quarks. A small mass splitting between the gluino and neutralino (χ_2^0) will result in low p_T quarks and a high p_T neutralino χ_2^0. This neutralino χ_2^0 further decays into another neutralino χ_1^0 with the emission of a Higgs or Z boson. The neutralino χ_1^0 escapes detection.

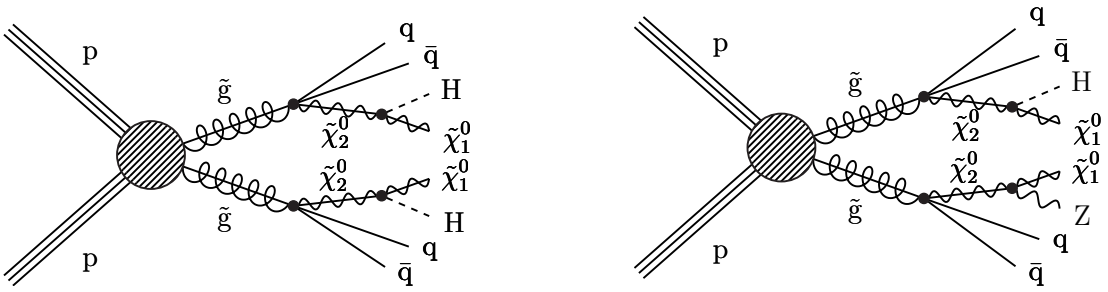

(a) The T5HH model. (b) The T5ZH model.

Figure 4.1: A diagram of the SMS models used for interpretations of this analysis.

The most salient selection criteria is the requirement of at least two high-p_T (¿ 300 GeV) AK8 jets.

4.3 Background estimation

The background estimation procedure makes use of what is known as an "ABCD" prediction where the analysis phase space is divided up into signal and sideband regions using scaling relations to make predictions of the Standard Model background inclusive in all processes. The phase space is divided up according to whether or not the jets are a) in the signal mass region and b) have been tagged as being consistent with a $b\bar{b}$ jet. A diagram of this partitioning is seen in Figure **??**. The two signal regions A_1 and A_2 contain events with one (and only one) or two jets being consistent with Higgs boson decay. Assuming that there is no correlation between the jet mass and

the $b\bar{b}$-tagging, the ratio of events $A_{1,2}/B_{1,2}$ should be the same as C/D. Rearranging this gives a prediction for the events in the A1 or A2 signal regions, $(A_{1,2})_{\text{prediction}} = (B_{1,2} * C/D)_{\text{observed}}$. The signal regions in data are blinded until the background prediction is made, but we are able to test the closure of our background estimation method in simulation. The closure is seen in Figure **??**. To account for the non-closure in the signal regions in data a correction factor κ is applied to each prediction. The values of κ are calculated from a combination of data and simulation. The values can be seen in Table **??**.

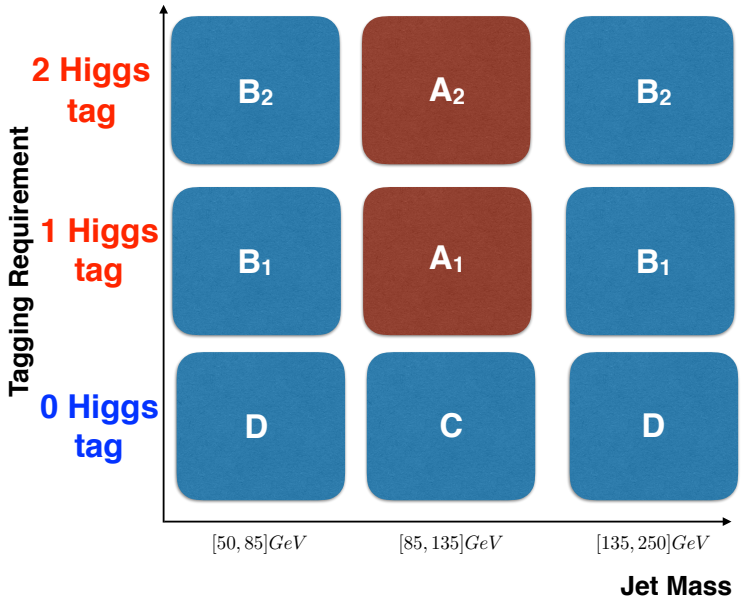

Figure 4.2: A diagram of the partitioned phase space.

Yields in these control regions are seen in Figure **??**.

4.4 Results

Observed yields in the two signal regions (A1 & A2) are seen in Figure **??**. The yields in the signal and control regions, along with the background predictions, are seen in Table **??**. Our signal region yields are consistent with the background expectation.

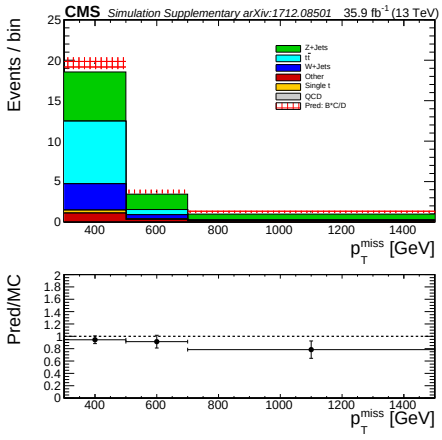

(a) The single Higgs tag region (A_1).

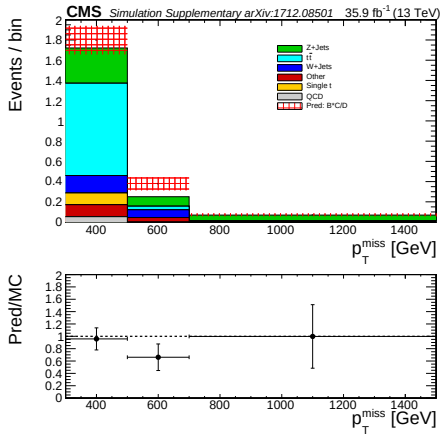

(b) The double Higgs tag region (A_2).

Figure 4.3: Simulation-based closure in the signal regions.

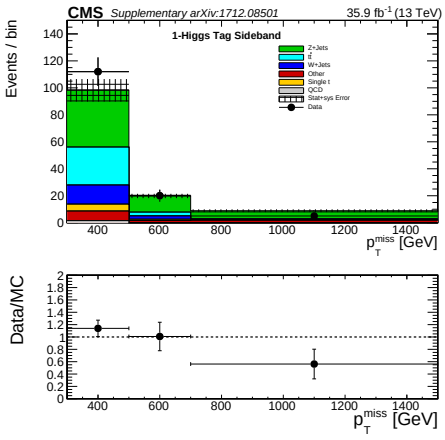

(a) B1

figs/Unblinding_doubletagSB.pdf

(b) B2

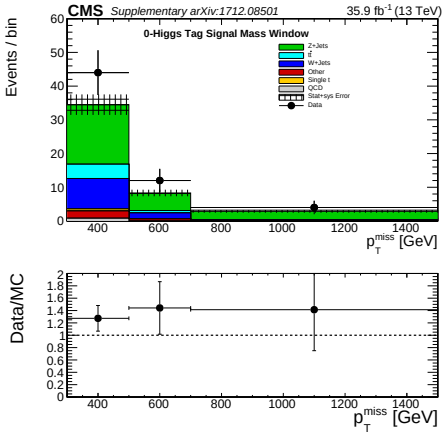

(c) C

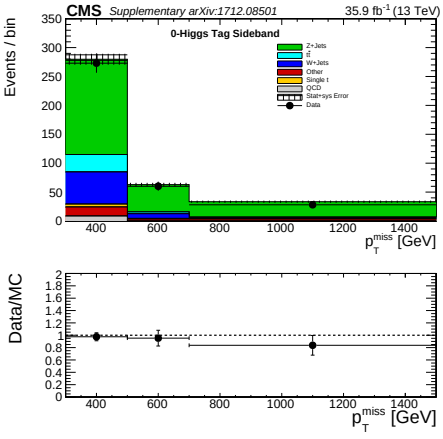

(d) D

Figure 4.4: Observed yields in the four control regions.

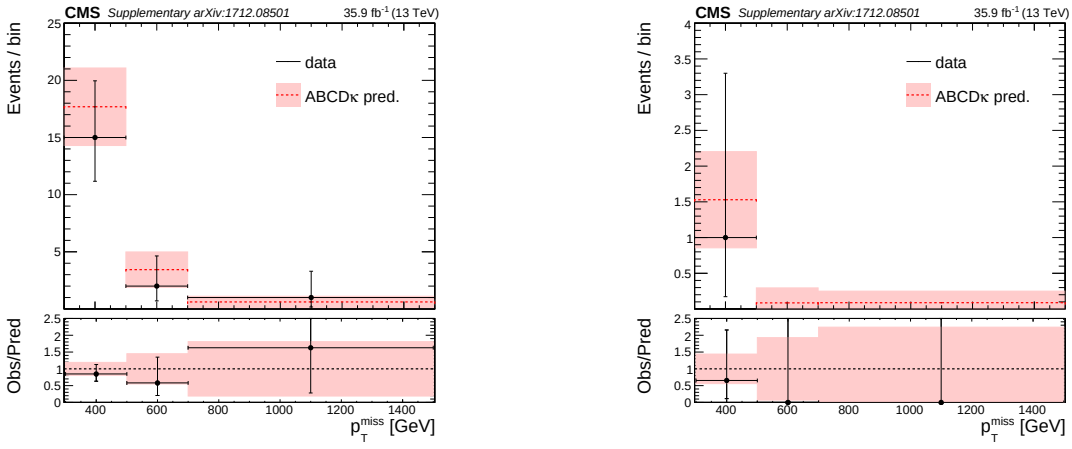

(a) One Higgs tag (A1)

(b) Two Higgs tag (A2)

Figure 4.5: Observed yields in the single and double Higgs-tagged signal regions.

Table 4.1: Observed yields in signal and control regions, along with the background predictions.

N_{H}	p_T^{miss} (GeV)	κ	$\mathrm{A}_{\mathrm{predicted}}$	A	B	C	D
1	300 – 500	0.98 ± 0.11	17.7 ± 3.8	15	112	44	273
1	500 – 700	0.86 ± 0.16	3.4 ± 1.5	2	20	12	60
1	>700	0.86 ± 0.17	0.61 ± 0.45	1	5	4	28
2	300 – 500	0.73 ± 0.14	1.52 ± 0.57	1	13	44	273
2	500 – 700	0.43 ± 0.12	0.09 ± 0.08	0	1	12	60
2	>700	0.62 ± 0.30	$0.09\ ^{+0.11}_{-0.09}$	0	1	4	28

Interpreting our results in the context of the T5HH or T5ZH models, the absence of signal allows us to place limits on the masses of the Supersymmetric particles. Assuming a mass of 1 GeV for the neutralino χ_1^0, and a small mass splitting of 50 GeV between the gluino and neutralino χ_2^0, we are able to place lower limits at 95% confidence level on the gluino mass at 2010 and 1825 GeV for the T5HH and T5ZH models, respectively. The exclusion curves are seen in Figure **??**. The weaker limit for the T5ZH model is due to the smaller branching fraction of the Z boson to b-quarks and our choice of signal mass window not being optimal for a Z boson.

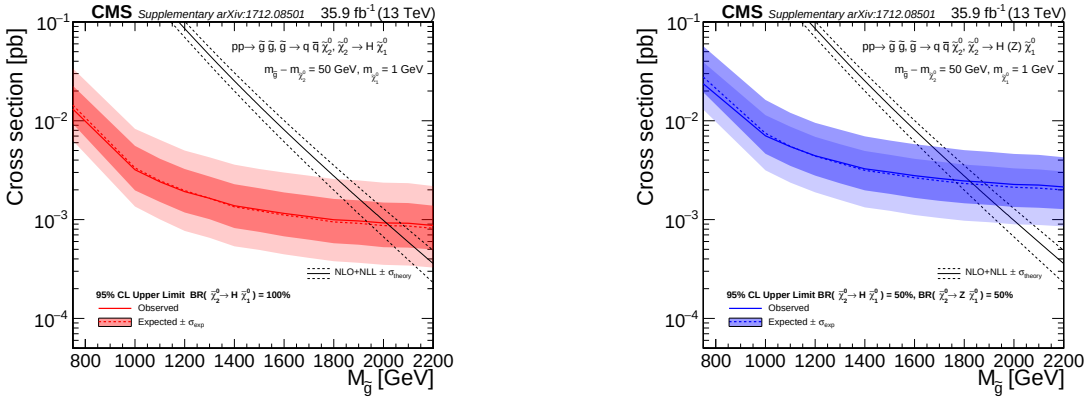

(a) The T5HH model.

(b) The T5ZH model.

Figure 4.6: Observed and expected limits on the gluino cross section when the data are interpreted in the context of our models.

4.5 Future Directions of this Analysis

Data collected at

Chapter 5

Conclusions

A chapter describing the conclusions.

Bibliography

[1] M. Cacciari, G. P. Salam, and G. Soyez, "The anti- k t jet clustering algorithm," Journal of High Energy Physics, vol. 2008, no. 04, p. 063, 2008.

[2] CMS Collaboration, "Search for supersymmetry in the multijet and missing transverse momentum final state in pp collisions at 13 TeV," Physics Letters B, vol. 758, pp. 152 – 180, 2016.

[3] CMS Collaboration, "Search for supersymmetry in multijet events with missing transverse momentum in proton-proton collisions at 13 TeV," Phys. Rev. D, vol. 96, p. 032003, Aug 2017.

[4] CMS Collaboration, "Search for physics beyond the standard model in events with high-momentum Higgs bosons and missing transverse momentum in proton-proton collisions at 13 TeV," 2017.

[5] S. D. Ellis, C. K. Vermilion, and J. R. Walsh, "Recombination algorithms and jet substructure: Pruning as a tool for heavy particle searches," Phys. Rev. D, vol. 81, p. 094023, May 2010.

Appendix A

$b\bar{b}$-tagging in Run 2017 data

This is a chapter detailing the commissioning of the $b\bar{b}$-tagging in Run 2017 data.